Retrospective Examination of Relative Permeability Data on Steady-State Two-Phase Flow in Porous Media

Marios Valavanides[1,a], Eraldo Totaj[1,b] and Minas Tsokopoulos[1,c]

[1]Department of Civil Engineering, TEI Athens, Ag. Spyridonos, GR-12210 Greece

[a]marval@teiath.gr, [b]aldo.totaj@yahoo.com, [c]minas.tso@gmail.com

Keywords: Two-phase flow, porous media, steady-state, operational efficiency

Abstract. Experimental evidence on the phenomenology of steady-state two-phase flow in porous media processes is recorded in the well-known relative permeability diagrams published in the literature. In the present work, the preliminary results of an extensive retrospective examination comprising a total of 88 published relative permeability diagrams, pertaining to a variety of steady-state two-phase flow conditions and types of porous media, are presented. Relative permeability data sets cropped from these diagrams were transformed into process operational efficiency data sets. Operational efficiency is considered as the ratio of oil transport over mechanical power supplied to the process ("oil produced per kW dissipated in pumps"). The re-examination revealed a universal, latent process characteristic: the existence of optimum operating conditions, i.e. conditions whereby process efficiency attains a maximum value. Its appearance and its correlation with the process conditions merit further investigation.

Introduction

Two-phase flow in porous media is a physical process whereby a wetting phase ("water") displaces a non-wetting phase ("oil") within a porous medium. It occupies a central position in physically important processes with practical applications of industrial and environmental interest, such as enhanced oil recovery, groundwater and soil contamination and subsurface restoration, the operation of multiphase trickle-bed reactors, the operation of proton exchange membrane fuel cells (PEMFC), etc. The majority of those applications are based on inherently transient processes. Nevertheless, to understand the physics of such processes in a deeper context, we need first to understand the stationary case, steady-state flow in macroscopically homogeneous p.m. or pore networks, whereby the two immiscible phases, "oil" & "water", are forced to flow at pre-selected, constant flowrates.

The concept of relative permeability is basic when the two immiscible phases flow simultaneously within a porous medium. It has been contrived to extend Darcy's law in accounting the phenomenology of the process. The, so-called, fractional Darcy's law takes the form

$$\tilde{U}_i = k_{ri}\,\frac{\tilde{k}}{\tilde{\mu}_i}\left(-\frac{\Delta\tilde{p}}{\Delta\tilde{z}}\right)_i \qquad i = o, w \tag{1}$$

where $\tilde{U}_o$ and $\tilde{U}_w$ are the superficial velocities of "oil" (the non-wetting phase = "o") and "water" (the wetting phase – "w"), e.g. oil/water, gas/oil, etc; $\tilde{\mu}_o, \tilde{\mu}_w$ are the dynamic viscosities of the two

phases and $\left(-\Delta\tilde{p}/\Delta\tilde{z}\right)_i$ represents the macroscopic pressure gradient in each phase, $i = o, w$. The relative permeabilities of oil and water (dimensionless variables) are denoted by k_{ro} and k_{rw} respectively. *Note*: In this paper, a tilde (~) denotes a dimensional variable.

In general, relative permeabilities are measured either by *steady-state* or *unsteady-state* methods (for a brief review of the methods commonly used to determine relative permeability, see Honarpour *et al.* [1]). In steady-state methods, the two-phases are simultaneously injected at a fixed ratio into a porous medium. When the system reaches steady-state conditions, the differential pressure and the saturation (by convention) of the wetting phase, S_w, are measured and the relative permeabilities can be calculated by using Darcy's law, eqn. (1). Steady-state methods are in general relatively accurate, easy to understand and implement straightforward and acceptable data processing procedures, namely regular/special core analysis. However, since the process needs to reach steady-state conditions it is, in general, time-consuming. Relative permeability curves are produced for a given porous medium and for a given pair of fluids by laboratory measurements when different flow conditions are imposed.

Diagrams of relative permeability for oil and water provide valuable and necessary data input in reservoir studies when estimating the producible reserves and the ultimate recovery. Nevertheless, we must point out that, at present, pragmatic sustainability issues on energy production/management (hydrocarbons, fuel cells, catalytic or trickle-bed reactors) shifted "recovery optimization" trends into "process efficiency optimization" scopes and targets. As a consequence, new challenges emerge within a wide spectrum of technological problems, extending from laboratory to industrial scale, e.g. unconventional/ enhanced oil recovery /carbon capture & sequestration processes, soil and aquifer pollution & remediation, operation of trickle-bed reactors [2]. To address these issues we need first to examine if any efficiency characteristics are inherent in the sought process, starting from its simpler form, immiscible steady-state.

The scope of the present work is to collect data from laboratory studies of steady-state two-phase flow in porous media, in order to examine if operational characteristics of such processes show a universal trend and, if that trend can be exploited in a systematic way.

Operational Efficiency Aspects of Two-Phase Flow in Porous Media

Consider the simultaneous flow of oil and water through a pore network. In order to induce and sustain specific flowrates of oil, $\tilde{q}_o$, and water, $\tilde{q}_w$, corresponding pressure differences, $\Delta\tilde{p}_o$ and $\Delta\tilde{p}_w$, must be effected upon the two phases. Consequently, an amount of mechanical power, $\tilde{W}$,

$$\tilde{W} = \tilde{q}_o \Delta\tilde{p}_o + \tilde{q}_w \Delta\tilde{p}_w \tag{2}$$

must be externally supplied to the system to balance the rate of mechanical energy dissipation within the process. The later is caused interstitially (a) by bulk viscous stresses in combination with the local rates of deformation, and, (b) by the velocities of moving menisci moving against local capillary pressure differences induced by contact angle hysteresis. The relative magnitude of the two contributions depends -among other factors- on the degree of disconnection of oil.

The reduced rate of mechanical energy dissipation, W, is defined as [3]

$$W = \frac{\tilde{W}}{\tilde{W}^{1\Phi}} = \tilde{W}\frac{\tilde{k}\tilde{\mu}_w}{\left(\tilde{\gamma}_{ow}Ca\right)^2} \tag{3}$$

where $\tilde{W}^{1\Phi}$ equals the rate of mechanical energy dissipation of the equivalent one phase flow of water at a rate $\tilde{q}^{1\Phi} = \tilde{q}^{o} + \tilde{q}^{w}$. $Ca = \tilde{\mu}_w \tilde{U}_w / \tilde{\gamma}_{ow}$ is the capillary number, $\tilde{\gamma}_{ow}$ the interfacial tension between the two phases and $r = \tilde{q}_o / \tilde{q}_w = \tilde{U}_o / \tilde{U}_w$ is the oil-water flowrate ratio. The value of Ca provides a measure of the viscous forces over the capillary forces. Ca and r, comprise the essential independent variables of the process (also called *operational parameters*) [3].

The efficiency of the process, with respect to the oil transport over the mechanical power supplied to it or "oil produced per kW of mechanical power dissipated in pumps", may be assessed by the values of the energy utilization coefficient, f_{EU}, a macroscopic quantity originally defined by Valavanides & Payatakes in the context of the development of the *DeProF* mechanistic model [3], as

$$f_{EU} = \frac{r}{W(Ca, r)} \tag{4}$$

The mechanistic model *DeProF* for immiscible steady-state two-phase flow in pore networks [3], predicts the relative permeability of each phase using the concept of decomposition in prototype flows. It combines effective medium theory with appropriate expressions for pore-to-macro scale consistency for oil and water mass transport and takes into account the pore-scale mechanisms and the network-wide cooperative effects as well as the sources of non-linearity, caused by the motion of interfaces and other complex effects. Using the *DeProF* model, one can obtain the solution to the problem of steady-state two-phase flow in porous media in terms of the capillary number, Ca, the oil/water flowrate ratio, r, the oil/water viscosity ratio, $\kappa = \tilde{\mu}_o / \tilde{\mu}_w$, the advancing and receding contact angles, and a parameter vector, comprising not only the absolute permeability but also dimensionless parameters describing geometrical and topological characteristics of the porous medium affecting the flow (the latter are regarded as the *system parameters*).

Extensive simulations using the *DeProF* model algorithm revealed that a continuous line, r*(Ca), exists in the (Ca, r) domain for which the energy utilization index takes locally maximum values. This line appears when the ridge of the f_{EU}(Ca,r) surface is projected on the (Ca, r) plane, see Fig. 1, whereby the effect of Ca and r on the energy utilization index, f_{EU}, is depicted by "mountain-range" or "half-croissant" shaped surfaces).

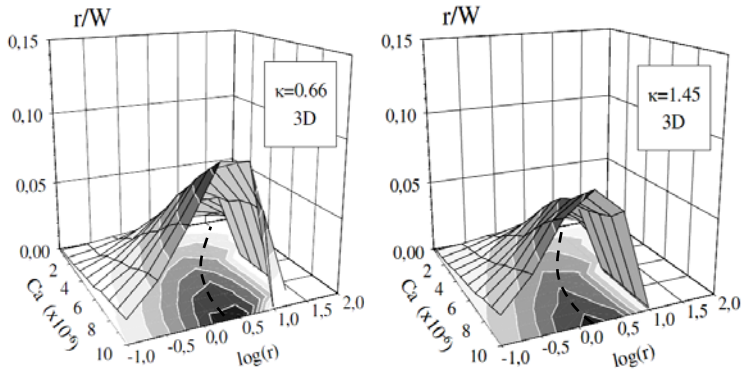

Fig 1. Energy utilization factor, f_{EU}=r/W, as a function of Ca and r. The diagrams pertain to 3D pore network *DeProF* simulations for two o/w systems with viscosity ratios $\kappa = 0{,}66$ and 1,45 [3]. Dashed lines represent the projection of the ridge of the f_{EU}(Ca,r) surface on the (Ca,r) planeeasurement of RCSP and patient charts

The existence of 'optimum conditions' for oil transport in two-phase flow in pore networks is a consequence of the remarkable internal adaptability of the flow to externally imposed flow constraints (Ca, r) and its inherent characteristic in self adjusting the connected versus disconnected moving-oil

balance. Detecting and setting such conditions is of ample importance in real processes of industrial scale. It is therefore imperative to challenge the *DeProF* theory claims regarding the existence of optimum operating conditions (OOC) in such processes and in the course of the present work we will provide the necessary experimental evidence. To this end, relative permeability diagrams for steady-state two-phase flow in porous media published in the literature are examined.

Transformation of Relative Permeability Data into Operational Efficiency Data

The transformation originally introduced by Valavanides [3] for steady-state two-phase flows in porous media,

$$r = \frac{\tilde{q}_o}{\tilde{q}_w} = \frac{\tilde{U}_o}{\tilde{U}_w} = \frac{k_{ro}/\tilde{\mu}_o}{k_{rw}/\tilde{\mu}_w} = \frac{1}{\kappa}\frac{k_{ro}}{k_{rw}} \qquad \& \qquad f_{EU} = \frac{k_{ro}}{\kappa(r+1)} = \frac{rk_{rw}}{r+1} = k_{ro}\left(\frac{k_{ro}}{k_{rw}} + \kappa\right)^{-1} \quad (5)$$

where $\kappa = \tilde{\mu}_o/\tilde{\mu}_w$ is the oil/water viscosity ratio, is valid for steady-state flow conditions. It was implemented in reconstructing measured relative permeability vs saturation data sets, $\{k_{ro}, k_{rw}, S_w\}$, into corresponding energy utilization vs flowrate ratio data sets, $\{f_{EU}, r\}$. The proof of eqns (5) is based on the observation that in steady-state conditions, the pressure gradient is the same in both phases, or, equivalently, the mobility ratio equals the flowrate ratio ([3], [6]).

Table 1. Classification of the re-examined laboratory studies [4-27] pertaining to a variety of steady-state flows in sand packs, plug cores, glass micromodels and virtual p.m. and fluid systems.

Core plug type	**Lab runs**
Berea sandstone	36
Carbonate core	3
Glass (incl. Pyrex™) pore network models	15
Loudon core	3
Teflon (consolidated, porous)	3
Propant pack	2
Bentheimer	2
Clashach sandstone	1
Virtual cores (L-B or CFD simulations)	19
Outcrop chalk	2
Pyrex (crushed)	2
In total	**88**

Viscosity ratio $\kappa = \tilde{\mu}_o/\tilde{\mu}_w$	**Lab runs**
Favorable, $\kappa < 1$	31
$\kappa = 1$	8
Unfavorable, $1 < \kappa$	48
Undisclosed	1
In total	**88**

Constant Ca runs	**53**

By using eqs. (5), reconstructions of $\{k_{ro}, k_{rw}, S_w\}$, into $\{f_{EU}, r\}$ data sets were produced for a total of 88 steady-state relative permeability diagrams from 24 published laboratory studies [4-27]. The re-examined systems and flow conditions examined have been coarsely classified in Table 1, whereas representative diagrams are presented in Figs. 2, 3 and 4.

The typical reconstruction of $\{k_{ro}, k_{rw}, S_w\}$, into $\{f_{EU}, r\}$ data sets is presented in Fig. 2, whereby steady-state relative permeability diagrams published in [4] & [10], are transformed into energy utilization diagrams.

ISBN: 978-1-61804-295-8

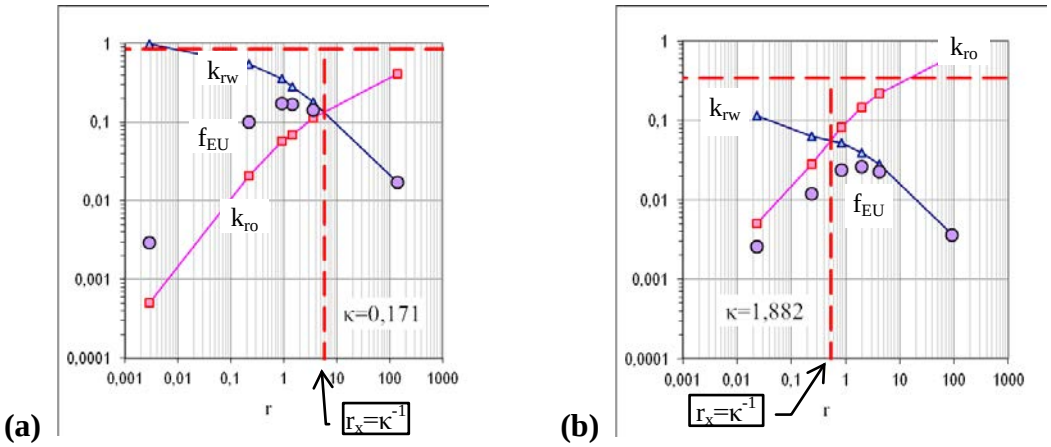

Fig. 2: Typical data sets of relative permeabilities for oil, k_{ro} (▫), & water, k_{rw} (▵) and energy utilization index, f_{EU}, (○) against flowrate ratio, r. The values of r & f_{EU} -computed through eqs (5) from source data- pertain to two typical systems: **(a)** favorable viscosity ratio in Berea sandstone [10] and **(b)** unfavorable viscosity ratio, in Clashach sandstone [4].

Results

The source relative permeability diagrams that were re-examined, together with the corresponding extracted data values and the diagrams produced from these data -when transformed by eqs. (5)- have been systematically recorded in a technical report (*ImproDeProF* project report, [28]). Here, the most representative diagrams are presented in Figs. 2, 3 and 4.

Referring to Figs. 2 - 4, the relative permeability data, k_{ri}, i=o,w and the corresponding logr and f_{EU} values, have been plotted together in appropriate (log-log) diagrams. Every set of {f_{EU}, logr} values, corresponding - through transformation eqs. (5)- to a {k_{ro}, k_{rw}} data set, presents a local maximum.

The majority of the examined relative permeability diagrams may be transformed into diagrams appearing as slide-cuts or curved-slice-cuts of surface diagrams similar to the f_{EU}(Ca, logr) diagrams predicted by the *DeProF* model (Fig. 1). In our review we found a few exceptional cases where there is either a lack of sufficient data, or, the original study was performed over a narrow span of flow conditions and optimum operating conditions have not been reached.

In all of the re-examined diagrams (Figs. 2 - 4 and [28]) the following trends are observed:

(a) Depending on the imposed flow conditions, the operational efficiency may vary by even two orders of magnitude. Optimum operating conditions, r*, are smooth functions of r in all diagrams and optimum operational efficiency can be reached in a smooth and continuous manner – there are no peaks or abrupt changes in f_{EU} with changes in r. Both attributes are of paramount importance when process efficiency is considered for industrial scale applications.

(b) Optimum operation conditions, r*, seem to depend primarily on the viscosity ratio, κ. The effect of other physicochemical parameters, e.g. wettability, porous medium structure is less obvious; to this end a systematic laboratory study should be designed.

(c) The dashed vertical line (in red) indicates the critical flowrate, r_x, for which the two relative permeabilities are equal. In all diagrams, the value of r_x is equal to the inverse of the viscosity ratio, $r_x = \kappa^{-1}$. The dashed horizontal line (in red) indicates the upper limit of the operational efficiency of the process, corresponding to pure viscous flow conditions ($Ca \to \infty$) [28].

(d) The flowrate ratio corresponding to the maximum value of f_{EU}, r*, is in general different than r_x. In systems with favorable viscosity ratios ($\kappa < 1$), $r^* < r_x$, whereas in systems with unfavorable viscosity ratios ($1 < \kappa$), $r_x < r^*$. The "distance" between these two figures, $|r^* - r_x|$, seem to correlate to the values of the system parameters and the imposed flow conditions.

ISBN: 978-1-61804-295-8

Favorable viscosity ratio, $\kappa = \tilde{\mu}_o / \tilde{\mu}_w < 1$

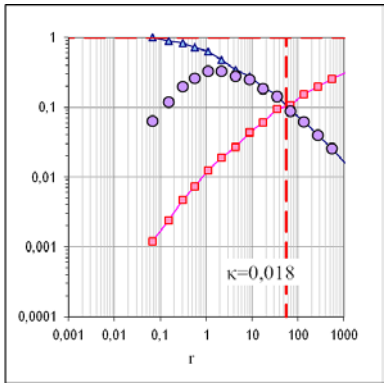

[19], fig. 4, "water/gas"

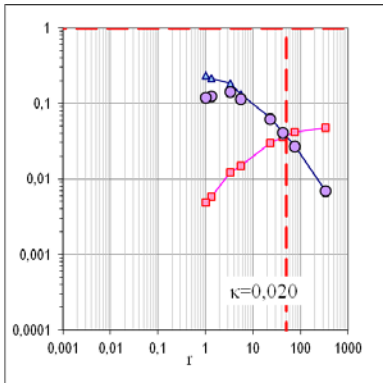

[12], fig. 5, "water/gas"

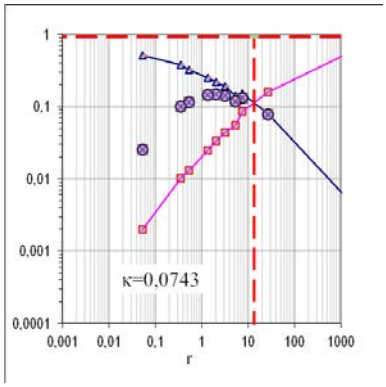

[20], fig. 4(b)

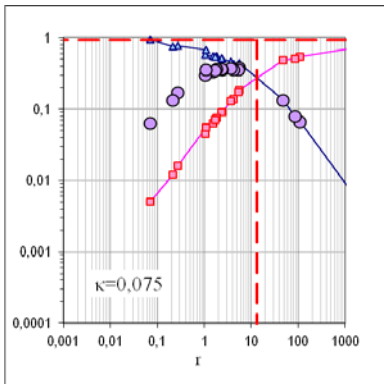

[7], fig. 2 "concurrent flow"

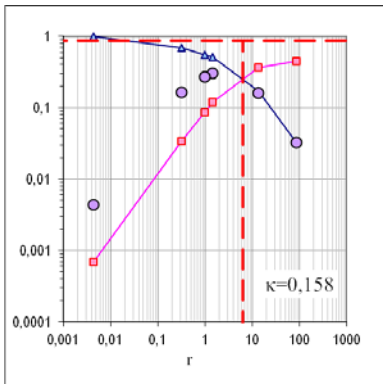

[10], fig.9, "run17"

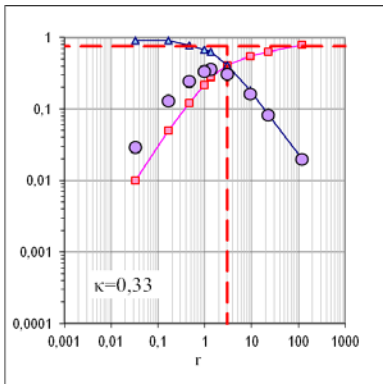

[11], fig.13, "neutr. wet, M=0,33"

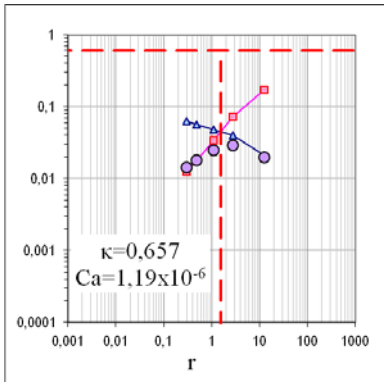

[5] "fig. 9(a)"

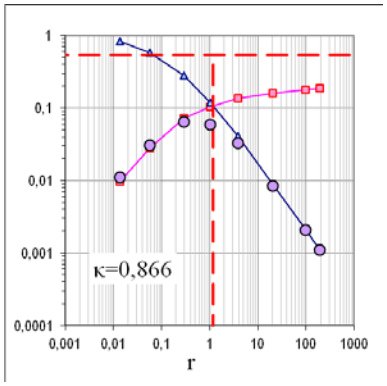

[25], fig. 2, "0,2cc/min"

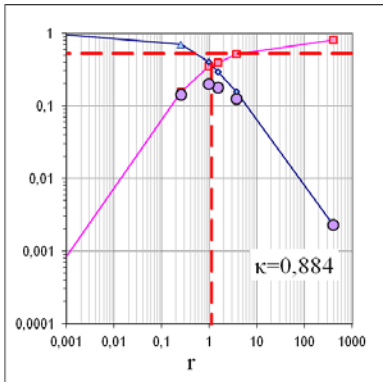

[10], fig. 5, "run11"

Fig. 3 Relative permeabilities for "oil" (▫) & "water" (△) and energy utilization index, f_{EU}, (○) against flowrate ratio, r, for "oil/water" systems with favorable viscosity ratios $\kappa = \tilde{\mu}_o / \tilde{\mu}_w < 1$ and for various flow conditions. Sub-legends refer source data.

ISBN: 978-1-61804-295-8

Unfavorable viscosity ratio, $1 < \kappa = \tilde{\mu}_o / \tilde{\mu}_w$

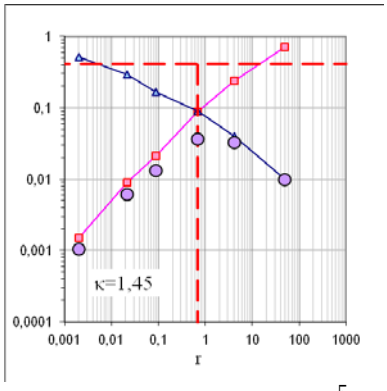

[13], figs 8 & 9 "Ca=10^{-5}"

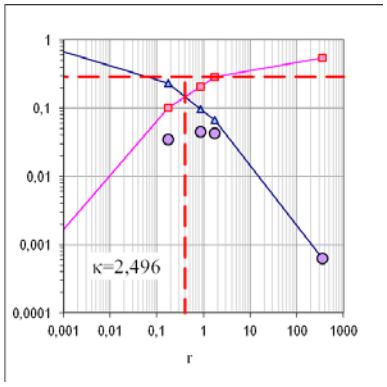

[10], fig. 4, "run 4"

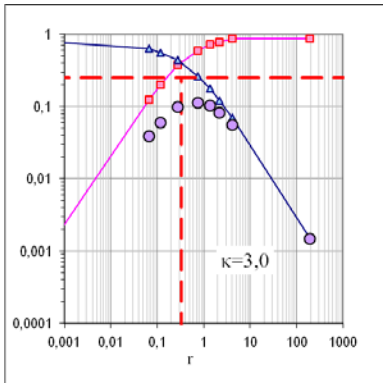

[11], fig. 13, "neutrally wet, M=3"

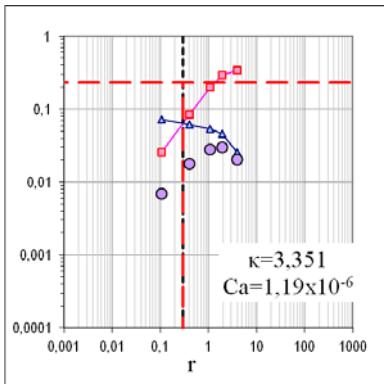

[5] "fig. 9(c)"

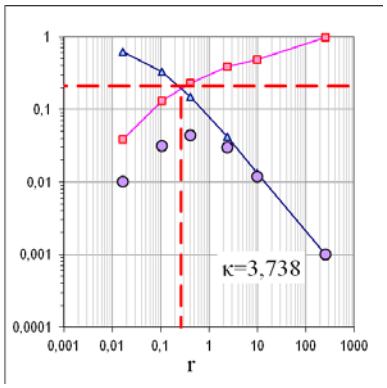

[27], fig. 3, "1st drainage"

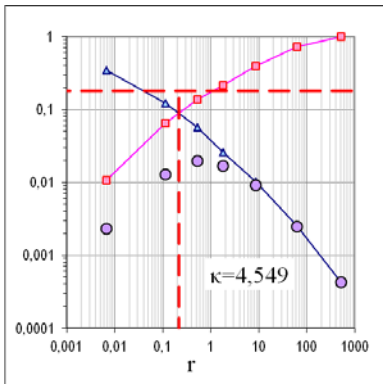

[9] fig.6, "incr. waterflood"

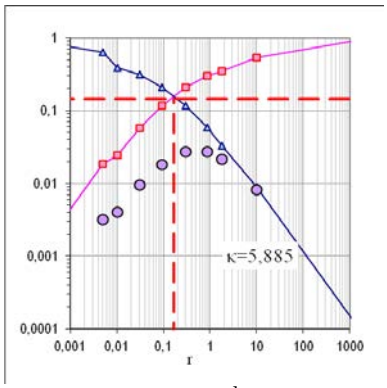

[17], fig. 14, "2nd drainage"

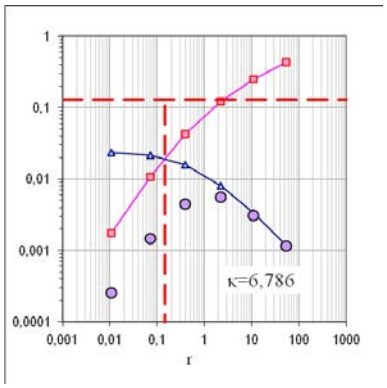

[8]

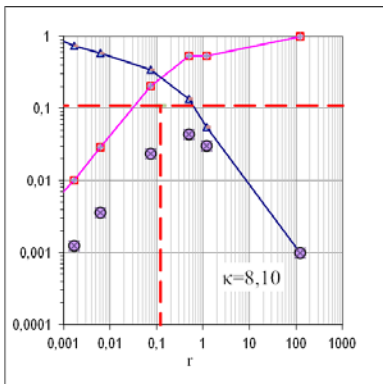

[24], fig. 3, "drainage"

Fig. 4 Relative permeabilities for "oil" (▫) & "water" (△) and energy utilization index, f_{EU}, (○) against flowrate ratio, r, for "oil/water" systems with unfavorable viscosity ratios $1 < \kappa = \tilde{\mu}_o / \tilde{\mu}_w$ and for various flow conditions. Sub-legends refer source data.

ISBN: 978-1-61804-295-8

Conclusions

An extensive –but not at all exhaustive- retrospective examination was performed comprising a total of 88 published relative permeability diagrams, pertaining to a variety of steady-state two-phase flow conditions and types of porous media. Each set of relative permeability data was transformed into a corresponding operational efficiency diagram. In all cases, a local maximum of the process operational efficiency for that particular system and for the set of flow conditions examined was obvious.

The trend of the measured values of (r, f_{EU}) corresponding to (k_{rw}, k_{ro}) is remarkably similar –not to say identical at this stage- to the trend of the f_{EU}(Ca,r) values predicted by the *DeProF* model/algorithm. Moreover, in general, the derived diagrams can be seen as lateral curved "slice" cut-outs of the f_{EU}(Ca,r) diagrams in Fig. 1; this is so because most of the relative permeability curves published in the literature are furnishing permeability measurements at steady-state conditions but at different values of the capillary number. This experimental evidence supports the universality of the *DeProF* theory findings with respect to the existence of optimum operating conditions in steady-state two-phase flow in porous media and reveals an opportunity of further deciphering the physics of the sought process.

Two-phase flow in p.m. is "burdened": (a) with oil disconnection and capillarity effects that restrain or inhibit -to a certain extent- the superficial transport of oil & water, (b) the bulk phase viscosities of oil & water. Process engineers can take advantage of these natural intrinsic characteristics and judge where to set the balance between capillarity or viscosity.

The results also indicate there is a potential for normative flow characterization, as to its capillary or viscous character, based on a few appropriately selected, non-dimensional physical variables. To do so, the conditions whereby process efficiency attains a maximum value and its correlation with the process characteristics (oil-water-porous medium system properties and flow conditions) merit a systematic investigation.

Acknowledgements

This research work has been co-funded by the European Union (European Social Fund) and Greek national resources in the frameworks of the "Archimedes III: Funding of Research Groups in TEI of Athens" (MIS 379389) research project of the "Education & Lifelong Learning" Operational Program.

References

[1] M. Honarpour, L. Koederitz, A.H. Harvey, *Relative Permeability of Petroleum Reservoirs*, Boca Raton, Florida, USA, CRC Press, 1986, ISBN 0-8493-5739-X

[2] M.S. Valavanides, C.D. Tsakiroglou, M.A. Ioannidis, O. Vizika, "Unconventional modelling of multi-phase flows in porous media", *Minisymposium 1.03, 7th International Conference on Porous Media*, Padova, Italy, May 18-21, 2015. Available: http://www.interpore.org/padova.

[3] M.S. Valavanides, "Steady-State Two-Phase Flow in Porous Media: Review of Progress in the Development of the *DeProF* Theory Bridging Pore- to Statistical Thermodynamics- Scales", *Oil & Gas Science and Technology*, vol. 67, pp. 787-804, 2012. Available: http://dx.doi.org/10.2516/ogst/2012056 .

[4] F.R. Allen, D.A. Pucket, "Theoretical and experimental studies of rate-dependent two-phase immiscible flow", SPE10972, AEE Winfrith, Dorset, U.K. (1986) pp. 62-74

[5] D.G. Avraam, A.C. Payatakes, "Flow Regimes and Relative Permeabilities during Steady-State Two-Phase Flow in Porous Media", *J. Fluid Mech*, vol. 293, pp. 207-236, 1995.

[6] D.G. Avraam, A.C. Payatakes, "Flow Mechanisms, Relative Permeabilities and Coupling Effects in Steady-State Two-Phase Flow in Porous Media. Case of Strong Wettability", *Industrial & Engineering Chemistry Research*, vol. 38, pp. 778-786, 1999.
[7] R.G. Bentsen, "Interfacial Coupling in Vertical, Two-Phase Flow Through Porous Media", *Journal of Petroleum Science & Technology*, vol. 23 pp. 1341-1380, 2005.
[8] E.M. Braun, R.J. Blackwell, "A steady-state technique for measuring oil-water relative permeability curves at reservoir conditions", SPE 10155 pp. 1-10, 1981.
[9] O.O. Eleri, A. Graue, A. Skauge, "Steady-state and unsteady-state two-phase relative permeability hysteresis and measurements of three-phase relative permeabilities using imaging techniques", SPE 30764, University of Bergen, Norway 1995, pp. 643-653.
[10] R.A. Fulcher, T. Ertekin, C.D. Stahl, "Effect of capillary number and its constituents on two-phase relative permeability curves", *Journal of Petroleum Technology*, vol. 37, pp 249-260, 1985.
[11] A. Ghassemi, A. Pak, "Numerical study of factors influencing relative permeabilities of two immiscible fluids flowing through porous media using lattice Botzmann method", *Journal of Petroleum Science and Engineering*, vol. 77, pp. 135–145, 2011
[12] B. Lai, J. Miskimins, "A new technique for accurately measuring two-phase relative permeability under non-Darcy flow conditions" SPE 134501, *ATCE2010*, Florence, Italy, 2010, pp. 1-14.
[13] H. Li, C. Pan, C.T. Miller, "Pore-scale investigation of viscous coupling effects for two-phase flow in porous media", *Phys. Rev. E*, vol. 72, no 26705, pp. 1-14, 2005.
[14] H.Y. Lo, N. Mungan, "Effect of temperature on water-oil relative permeabilities in oil-wet and water-wet systems", SPE 4505 Dallas, Texas (1973) pp. 1-12.
[15] D.G. Longeron, L. Cuiec, F.A. Yahya, "Water-oil relative permeabilities in the case of a mixed-wet carbonate reservoir: influence of experimental conditions", SCA 9324 *Annual Symposium of the Society of Core Analysts*, 1993, pp. 1-16.
[16] D. Maloney, K. Doggett, A. Brinkmeyer, "Special core analyses and relative permeability measurements on almond formation reservoir rocks" *NIPER*, vol. 648, pp. 1-30, 1993.
[17] S.K. Masalmeh, "The effect of wettability heterogeneity on capillary pressure and relative permeability", *Journal of Petroleum Science and Engineering*, vol. 39, pp. 399-408, 2003.
[18] J.E. Nordtvedt, H. Urkedal, A.T. Watson, E. Ebeloft, K. Kolltveit, K. Langaas, I.E.I. Oxnevad, "Estimation of relative permeability and capilary pressure functions using transient and equilibrium data from steady-state experiments", SCA 9418 *Annual Symposium of the Society of Core Analysts*, pp. 197-206, 1994.
[19] M.J. Oak, L.E. Baker, D.C. Thomas, "Three-phase relative permeability of berea sandstone", *Journal of Petroleum Technology*, vol. 42, pp. 1054-1061, 1990.
[20] J-C Perrin, M. Krause, C-W Kuo, L. Miljkovic, E. Charob, S.M. Benson, "Core-scale experimental study of relative permeability properties of CO2 and brine in reservoir rocks", *Energy Procedia*, vol. 1, pp. 3515-3522, 2009.
[21] T. Ramstad, N. Idowu, C. Nardi, P.E. Oren, "Relative permeability calculations from two-phase flow simulations directly on digital images of porous rocks", *Transport in Porous Media*, vol. 94, pp. 487-504, 2012.
[22] J.L. Shafer, E.M. Braun, A.C. Wood, J.M. Wooten, "Obtaining relative permeability data using a combination of steady-state and unsteady-state core floods", SCA 9009 *Annual Symposium of the Society of Core Analysts* Houston, Texas, 1990, pp. 1-16.
[23] Q. Sheng, K.E. Thompson, J.T Fredrich, P.A. Salino, "Numerical Prediction of Relative Permeability from MicroCT Images: Comparison of Steady-State versus Displacement Methods", SPE 147431 pp. 1-16, 2011.
[24] A.W. Talash, "Experimental and Calculated Relative Permeability Data for Systems Containing Tension Additives", AIME SPE5810, pp. 177-188, 1976.

[25] G.A. Virnovsky, Y. Guo, S.M. Skjaeveland, P. Ingsoy, "Steady-state relative permeability measurements and interpretation with account for capillary effects", SCA 9502 *Annual Symposium of the Society of Core Analysts*, pp. 1-10, 1995.
[26] V.A. Virnovsky, K.O. Vatne, S.M. Skjaeveland, A. Lohne, "Implementation of multirate technique to measure relative permeabilities accounting for capillary effects", SPE 49321, New Orleans, Louisiana, pp. 901-911, 1998.
[27] F.H.L. Wang, "Effect of wettability alteration on water/oil relative permeability dispersion and flowable saturation in porous media", *SPERE* 15019, pp. 617-628, 1988.
[28] M.S. Valavanides, E. Totaj, M. Tsokopoulos, "Retrospective Examination of Relative Permeability Data on Steady-State 2-Ph Flow in Porous Media Transformation of Rel-Perm Data (k_{ro}, k_{rw}) into Operational Efficiency Data (f_{EU})", ImproDeProF /Archimedes III, project internal report, 2014. Available: http://users.teiath.gr/marval/ArchIII/retrorelperm.pdf